ISBN: 978-628-96613-1-6. ISSN: 2414-6390. Digital Object Identifier: https://dx.doi.org/10.18687/LACCEI2025.1.1.1081

A comparison of neural networks for prediction of generation of thermal energy of Flat Plate Vacuum solar thermal collectors

Elmer Arellanos-Tafur [1,2,5], Felix Rojas-Arquiñego[3] and Marcelo Damas-Niño[4]
[1] Universidad Tecnológica del Perú, Peru, c19083@utp.edu.pe
[2] Universidad de Ingenieria y Tecnologia - UTEC, Peru, earellanos@utec.edu.pe
[3] Universidad Señor de Sipan, Peru, felixrojas@uss.edu.pe
[4] Universidad Nacional del Callao, Peru, mndamasn@unac.edu.pe
[5] Universidad Continental, Peru, earellanos@continental.edu.pe

***Abstract*—Solar thermal collectors are essential for sustainable energy production, yet accurately predicting their energy output remains challenging. This research compares the precision of three time series neural networks—NARX (Nonlinear Autoregressive with Exogenous Inputs), NAR (Nonlinear Autoregressive), and Input-Output models—for forecasting thermal energy generation y(t) from flat plate vacuum solar collectors based on time series data x(t). The objective was to determine which neural network architecture provides the highest reliability for energy output prediction, enabling more effective system management. Using a correlational design, each neural network was constructed with historical thermal energy and solar radiation data, then subjected to training, validation, and testing phases. Predictive accuracy was evaluated through linear regression analysis between network outputs and corresponding targets, quantifying how well each model could generalize to new data. Results revealed that the NARX model demonstrated superior overall performance with consistent high correlation coefficients across all phases. The Input-Output model showed exceptional accuracy particularly during the testing phase, suggesting strong practical reliability. The NAR model, while effective overall, exhibited reduced accuracy in the testing phase, indicating limitations in generalizing to unknown data. This study concludes that the NARX architecture provides the most stable and accurate framework for predicting thermal energy generation in flat plate vacuum solar collectors. These findings contribute to more effective planning of solar energy systems, optimization of resources, and improved maintenance scheduling, ultimately reducing operational costs and extending system component lifespans.**

Keywords: Network, prediction, thermal energy, collectors.

I. Introduction

The generation of energy from renewable sources has become increasingly important in the search for sustainable and clean alternatives to fossil fuels. In the present era, the energy demand proliferates worldwide due to population spurt and industrialization [1], [2]. Depleting fossil fuels, emission of greenhouse gases, and damage to the ecosystem have paved a path toward using emission-free renewable energy sources [3], [4]. Exploration of eco-friendly energy resources is the need of the future and solar technologies play a critical role as a solution to eco-friendly energy exploration [5]. Global average temperatures are rising due to the increasing amount of greenhouse gas emissions causing natural disasters and having negative impact to nature and humans [6]. As currently the largest share of CO2 emissions are caused by burning of fossil fuels, renewable energy sources are increasingly employed in order to reduce the carbon footprint of the primary energy sector [7]. However, with the integration of increasing amounts of renewable energy, the supply of energy is stronger varying due to the external dependencies of renewable energies, i.e. wind or sunshine [8]- [9]. Under the dual pressure of energy transition and environmental pollution, comprehensive utilization of renewable energy is the direction for the development of a diversified clean energy system [10]. Renewables are expected to grow by 2.3% each year [11], posing major operational challenges due to their stochastic nature [12]- [13]. All countries are forced to consider renewable energy systems to meet their increasing demands. Solar energy can be considered the most important renewable energy source due to its sustainability, friendly environment and vital availability. Therefore, the utilization of solar energy to meet the increasing demands of energy is becoming more urgent. The water heating sector, industrial applications and water desalination systems consume a considerable amount of energy. Using solar energy for water heating can save this amount of energy utilized in these applications [14]. Achieving widespread use of renewable energy sources (RES) is one of the most important targets of future power systems [15], [16]. Due to the intermittent and volatile characteristics of RES, it is too costly or even infeasible to balance the power supply and demand by only relying on the conventional units under significant RES penetration [17]. The uncertainty associated with renewable energy forecasting poses technical and economic challenges to the operation and management of power systems [18]. At the system operator level, the tasks such as reserve requirement determination [19], unit commitment, and economic dispatch [20] will be affected by the forecast accuracy [21]. Vacuum flat plate solar collectors represent an advanced technology

.

for the efficient conversion of solar radiation into thermal energy. However, the variability of solar radiation, influenced by atmospheric and meteorological conditions, poses a significant challenge for the accurate prediction of thermal energy output. In response to this challenge, artificial neural networks (ANNs) have emerged as effective tools for modeling and forecasting time series in complex systems, owing to their ability to capture nonlinear relationships and uncover hidden patterns in the data. Among the most relevant ANN models are the Nonlinear Autoregressive model with Exogenous Inputs (NARX), the Nonlinear Autoregressive model (NAR), and the Input-Output (I/O) model. The NARX model integrates external information, such as solar radiation, making it particularly suitable for scenarios where external factors have a significant impact. In contrast, the NAR model relies solely on the past values of the variable to be predicted, resulting in a simpler structure that may limit accuracy in complex environments. The I/O model offers a more flexible framework that can be adapted to various input-output configurations. This study presents a comparative analysis of the predictive accuracy of these three models in forecasting thermal energy generation from vacuum flat plate solar collectors, using a time series database that includes solar radiation and thermal energy data. The applied methodology involved data selection and preparation, neural network construction and training, as well as validation, testing, and accuracy assessment through linear regression analysis. The findings provide a comprehensive understanding of each model's performance and its practical and theoretical implications, contributing valuable insights for the optimization of solar thermal systems and the promotion of more efficient solar energy utilization.

II. Theoretical framework

A. Artificial neural networks and the prediction process

Artificial neural networks are a powerful tool for time series prediction due to their ability to model complex nonlinear relationships in data. Neural networks are inspired by the structure of the human brain and consist of layers of artificial neurons that process information. The following steps are followed in the prediction process with neural networks:

- Data preprocessing: This involves normalizing or standardizing the data, removing outliers, and creating features such as time delays that represent previous values in the series.
- Model training: The model is trained using a historical dataset, adjusting the network weights to minimize the prediction error.
- Validation and evaluation: A validation dataset is used to adjust hyperparameters and assess the model's performance on unseen data. Metrics such as Mean Squared Error (MSE) or Mean Absolute Error (MAE) are used.
- Prediction: Once trained and validated, the model is used to make future predictions.

B. NARX model

The NARX (Nonlinear Autoregressive with Exogenous Inputs) model is an advanced tool in predictive modeling that captures complex dynamics. NARX is a recurrent dynamic neural network architecture used to model input-output nonlinear systems. NARX uses the present input, past inputs and past outputs to model the dynamics of the nonlinear system [22]- [23]. The NARX model is particularly effective in scenarios where the system's behavior depends on both current and historical data, making it suitable for time series forecasting and system identification tasks. The general equation of the NARX model is expressed as [24]:

$$y(t) = f\left(y(t-1), y(t-2),..., y(t-n), u(t-1), u(t-2),..., u(t-m)\right) + (t)$$

where:

- y(t) is the dependent variable at time t
- y(t-i) are the past values of the dependent variable
- u(t-j) are the past exogenous inputs
- f is a nonlinear function that describes the relationship between the variables
- (t) is an error term

The function f can take various forms, including polynomial nonlinear models, neural networks, or any other function capable of capturing the complexity of the system.

C. NAR model

The NAR (Nonlinear Autoregressive) model is an advanced approach in predictive time series modeling that captures complex dynamics through nonlinear relationships between variables. Unlike linear autoregressive models that limit the ability to model nonlinear phenomena, the NAR model extends the traditional concept by incorporating a nonlinear function to represent the interactions between variables. As the NAR model employs the historical signals as the inputs, it can predict the motion scenarios with higher accuracy [25]. The NAR model is based on the premise that the dynamics of a time series can be represented by a nonlinear function of its past values. The general formulation of the NAR model is expressed as [26]:

$$y(t) = f\left(y(t-1), y(t-2),\ldots,y(t-n)\right) + (t)$$

where:

- y (t) is the output variable at time t
- y (t-i) represents the past observations of the output variable
- f is a nonlinear function that models the relationship between past values and the current value
- (t) is the random error term

The function f is the core of the NAR model, and its selection is crucial for accurately capturing the nonlinear dynamics of the system. This function can be represented in various ways, including polynomials, radial basis functions, or neural networks.

D. Nonlinear Input-Output model

The nonlinear input-output model is a fundamental tool in nonlinear systems theory, used to model and analyze complex phenomena across various disciplines. Nonlinear dynamic systems have proven to be ubiquitous in nature and engineering, ranging from fluid dynamics to molecular biology. Unlike linear systems, whose behaviors can be described using linear differential equations and superposition principles, nonlinear systems present additional complexities that require specialized methods for their analysis. The model is based on the premise that the relationship between a system's inputs and outputs cannot be adequately described by a linear function. Instead of using a linear equation, the model employs nonlinear functions to capture the system's dynamics. Mathematically, it can be expressed as [27]:

$$y(t) = f(x(t), u(t))$$

where y(t) is the system output, x(t) represents the internal state, and u(t) is the input. The function f is a nonlinear function that describes the relationship between the system's variables.

E. Vacuum flat plate solar thermal collectors

These devices are designed to capture solar radiation and convert it into thermal energy, which is used for applications such as water heating, space heating, and industrial processes. These collectors combine elements of traditional flat plate collectors with vacuum technology, commonly used in evacuated tube collectors, to enhance thermal efficiency and reduce heat losses. The operating principle of vacuum flat plate solar thermal collectors focuses on the efficient capture and conversion of solar energy into usable heat, optimizing each stage of the process to minimize energy losses. The operation of the vacuum flat plate solar thermal collector is mainly constituted by the following processes:

- Solar radiation capture: Solar radiation strikes the transparent cover of the collector and is transmitted almost unobstructed to the absorber plate due to the optical properties of the glass. The cover also reduces heat losses through convection and radiation, maintaining high efficiency in solar energy capture
- Conversion of solar energy into heat: The absorber plate, coated with a selective material, absorbs the solar radiation and converts it into heat. The selective coating is crucial for optimizing this conversion, as it maximizes solar radiation absorption while minimizing heat emission in the form of infrared radiation.
- Reduction of thermal losses: The heat generated in the absorber plate is efficiently retained thanks to the surrounding vacuum chamber, which acts as a superior thermal insulator. By eliminating the medium that would allow heat transfer through conduction and convection, the vacuum ensures that most of the heat remains within the system, allowing the plate to reach and maintain high temperatures with superior efficiency.
- Heat transfer to the working fluid: The accumulated heat is transferred to a working fluid that circulates through tubes or channels in contact with the absorber plate. This fluid, which can be water, thermal oil, or another suitable medium, transports the heat to a storage system or directly to the point of use.
- Heat storage and usage: The heat transferred to the working fluid can be used immediately for thermal applications or stored in thermal storage systems for later use. This allows for efficient and continuous utilization of thermal energy, even during periods without direct solar radiation, such as at night or on cloudy days.

Figure 1 shows the main parts of a flat plate solar thermal collector system, where its main parts are identified.

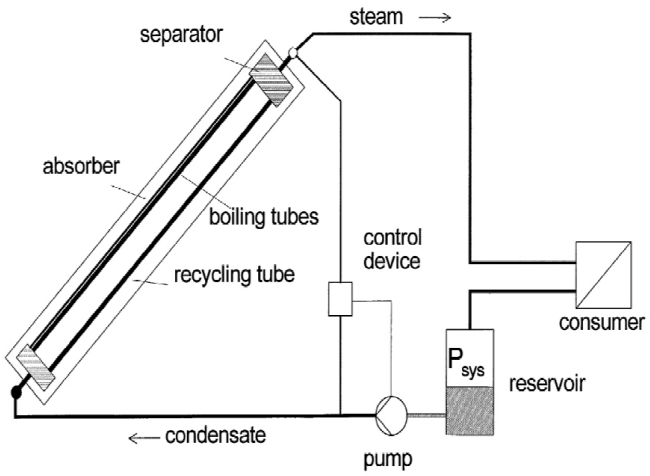

Fig. 1. Sketch of the flat plate solar thermal collector system [28]

F. Energy gain of a flat plate collector

It refers to the amount of solar radiation that the collector captures and converts into useful heat for thermal applications. The efficiency of the collector depends on factors such as the amount of incident solar radiation on the collector's surface area and the ability of the collector's surface to absorb that radiation. This absorption is not perfect, as some of the radiation is lost due to reflection, transmission through the collector material, or thermal emission. The conversion efficiency is influenced by the type of material used for the collector's surface, its absorptive capacity, and operating conditions such as the temperature of the absorber plate and available solar radiation. The energy gain is higher when the collector can efficiently absorb solar radiation and minimize losses, which depends on the collector's design, orientation, and the quality of materials used. The useful energy gain of a flat plate collector is given by [29]:

$$Q_u = SA_c - Q_{\text{loss}}$$

Where:

- Q_u: Useful energy gain

- S: Solar irradiation
- A_c: Collector area
- Q_{loss}: Energy losses

G. Energy loss of a flat plate collector

Energy losses mainly occur due to heat transfer to the surrounding environment. This process can occur through convection, where heat is transferred from the collector to the surrounding air, and through radiation, when the collector's surface emits heat to the glazing or directly to the air. As the temperature of the absorber plate increases, so do the thermal losses, as the temperature difference between the collector surface and the surrounding environment facilitates heat transfer. The design of the collector, such as the material of the absorbing surface and the properties of the protective glazing, also impacts the amount of energy lost. The greater the temperature difference between the collector and the environment, the higher the rate of heat loss, which decreases the overall efficiency of the system. Losses occur even if no heat is directly extracted from the collector, as heat is dissipated to the surroundings. Q_{loss} is due to energy loss through [30]:

$$Q_{\text{loss}} = U_L A_c (T_p - T_a)$$

where:

- U_L: Overall heat transfer coefficient based on collector area
- A_c: Collector area
- T_p: Mean temperature of the absorber plate
- T_a: Ambient temperature

The heat transfer coefficient at the top of the solar collector (U_t) describes how heat is transferred from the collector's surface to the fluid circulating inside the collector and to the surrounding environment. This coefficient is made up of two main components: heat transfer by convection between the absorber plate and the fluid, and heat transfer by radiation between the collector surface and the glazing or the surrounding air.

Figure 2 shows the heat transfer network along with the corresponding thermal resistance network. Where we have the following elements:

- $h_{c,p-g}$: Convective heat transfer coefficient between plate and glazing
- $h_{r,p-g}$: Radiative heat transfer coefficient between plate and glazing
- $h_{c,g-a}$: Convective heat transfer coefficient between glazing and ambient air
- $h_{r,g-a}$: Radiative heat transfer coefficient between glazing and ambient air

III. Methodology

A correlational design was considered to evaluate and compare the accuracy of different prediction models. Correlational design is particularly useful for identifying and quantifying the degree of relationship between these variables without the need to directly manipulate experimental conditions. In this context, the correlational design allows for the analysis of the relationship between the prediction level (dependent variable) y(t) and the implemented time series neural network model (independent variable) x(t) , using data such as previously generated thermal energy and solar radiation values received during the same period [31]; where the use or non use of these past values depended on the model being analyzed. For the prediction analysis of each model, the respective neural network was built using the required data, followed by training, validation, and testing phases to achieve the most accurate prediction possible. Then, through linear regression analysis between the network outputs and the corresponding targets, the results of the accuracy level for each stage were obtained, as well as the overall accuracy level. If the prediction were perfect, the network results and the targets would be exactly the same, but this relationship is rarely perfect in practice. The sequence of the implemented phases can be seen in Figure 3.

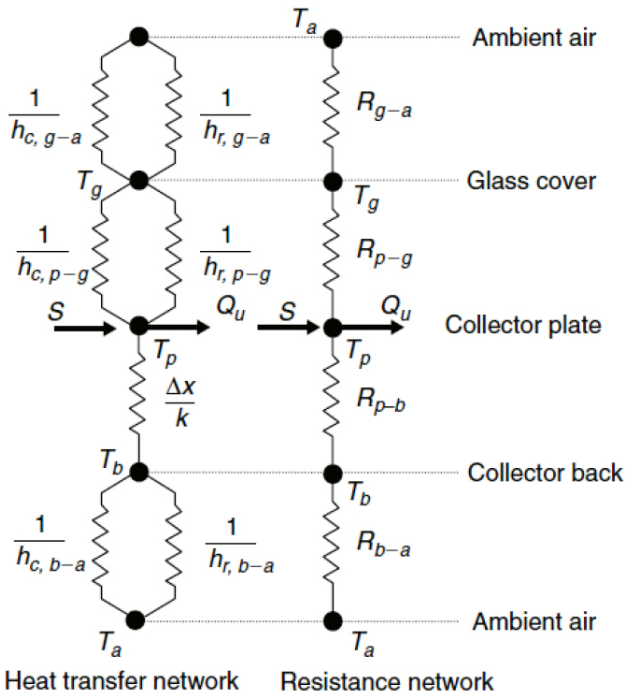

Fig. 2. Heat transfer network and resistance network

IV. Implementation and Results

The studied population consisted of a flat plate solar collector system specifically designed for thermal energy generation using vacuum insulation technology. This system represents a common configuration in renewable energy applications, where flat plate collectors are enhanced with vacuum layers to minimize heat loss and improve efficiency. See the details of system in Table I.

In the following lines we present the implementations and results for each model and at the end we have the final evaluation. Once the data collection phase was completed, the

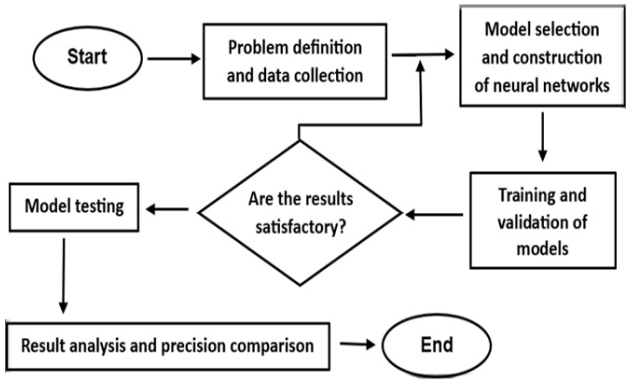

Fig. 3. Sequence of the implemented phases

TABLE I
STUDY POPULATION

Solar system	Characteristics	Location
Flat Plate vacuum Solar thermal Collector System	Composed of 50 flat plate vacuum solar thermal collectors, each with an area of 2 m².	Rooftop of the Betancourt building at the School of Engineering, Carlos III University of Madrid, Leganés, Spain.

data were coded and tabulated by recording the information obtained. The assigned data were divided as follows:

- 70% of the data were used for training, which indicated the degree of fit of the neural network for prediction.
- 15% of the data were used to conduct a completely independent test of the neural network's generalization.
- 15% of the data were used to validate that the neural network was generalizing properly.

The NARX network had a default sigmoid transfer function in the hidden layer and a linear transfer function in the output layer. There were two inputs: An external input and another feedback from the network output. For training, the network was configured with eight hidden neurons and two delays, as shown in Figure 4.

Figure 5 shows the performance of the NARX network until reaching the best value of the mean square error (MSE) at epoch 6, with the value of 1456.33.

Figure 6 illustrates the correlation coefficients in the different phases and the global correlation coefficient: 0.998.

The NAR network had a default sigmoid transfer function in the hidden layer and a linear transfer function in the output layer. The input values were the past data of the series to be predicted. For training, the network was configured with ten hidden neurons and two delays, as shown in Figure 7.

Figure 8 shows the performance of the NAR network, until reaching the best value of the mean square error (MSE) at epoch 9, with the value of 10515.1.

Figure 9 illustrates the correlation coefficients in the different phases and the global correlation coefficient: 0.996.

The nonlinear Input Output network had a default sigmoid transfer function in the hidden layer and a linear transfer function in the output layer. The input values were past data

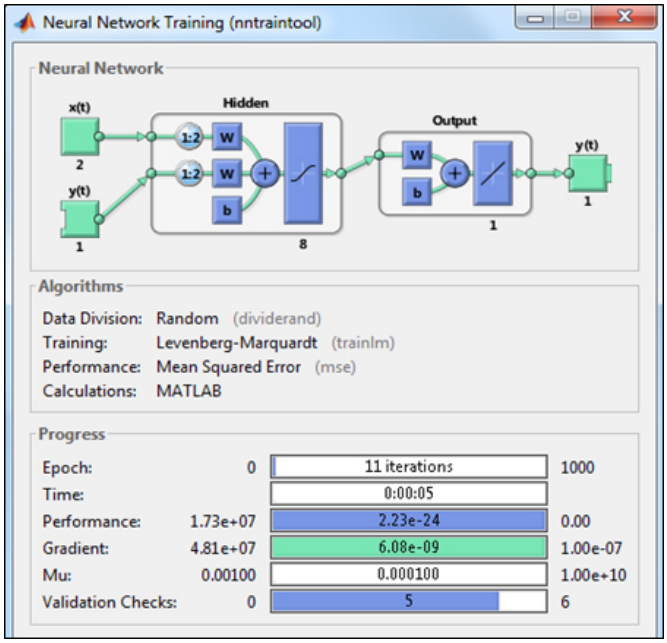

Fig. 4. NARX neural network training

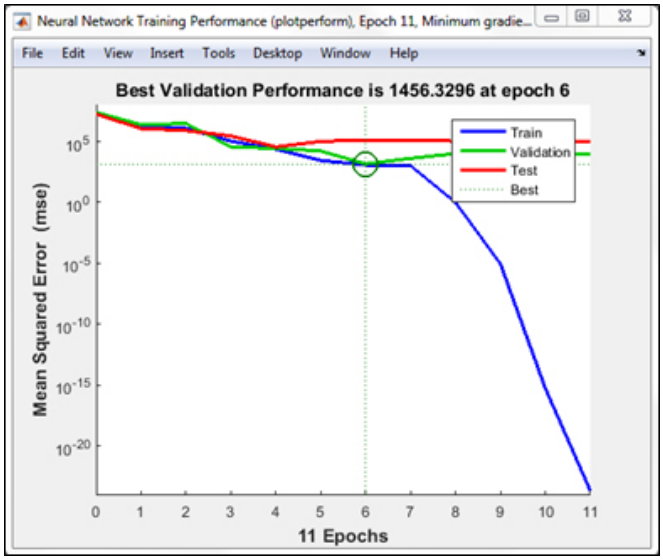

Fig. 5. NARX neural network performance

other than those of the series to be predicted. For training, the network was configured with ten hidden neurons and two delays, as shown in Figure 10.

Figure 11 shows the performance of the Input Output network, until reaching the best value of the mean square error (MSE) at epoch 2, with the value of 2656.32

Figure 12 illustrates the correlation coefficients in the different phases and the global correlation coefficient: 0.997.

Table II shows the results of the three neural network models, with the global correlation coefficient being the most significant value. Each value in the table indicates how well the variation in output is explained by the objectives. If this

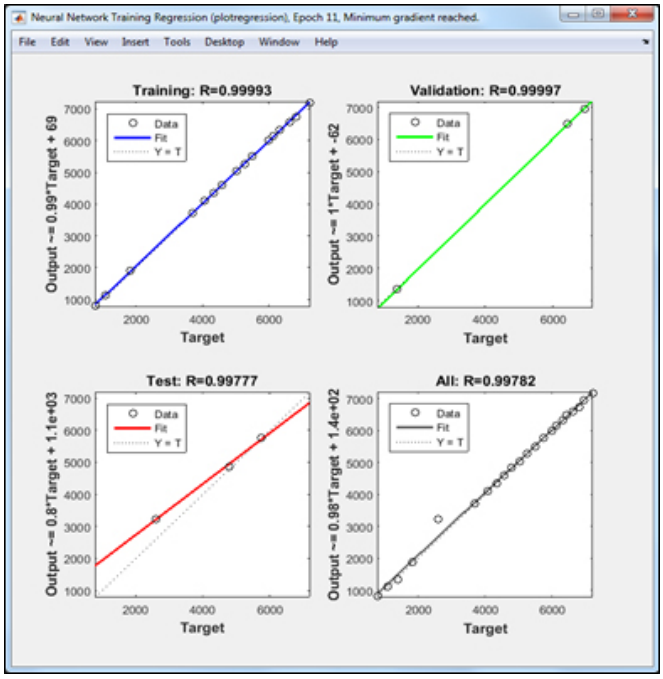

Fig. 6. Correlations of the NARX neural network

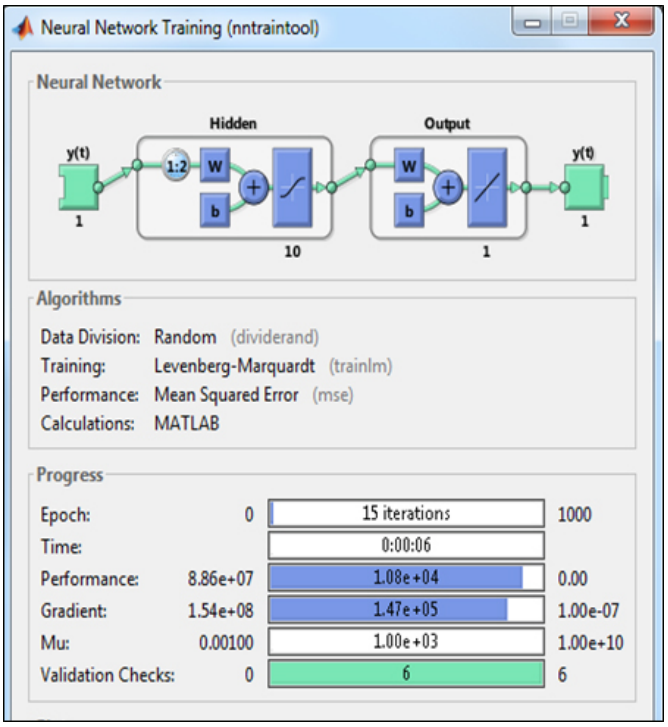

Fig. 7. NAR neural network training

number is equal to 1, then there is a perfect correlation between the objectives and the outputs. The general result obtained shows that the NARX model has a better level of prediction than the other two models.

Figure 13 shows how the correlation coefficients of the models vary across the phases. A slight decrease in the

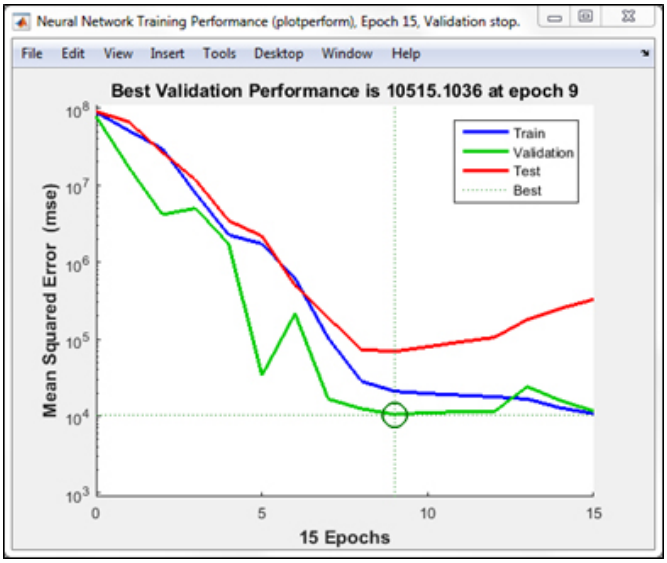

Fig. 8. NAR neural network performance

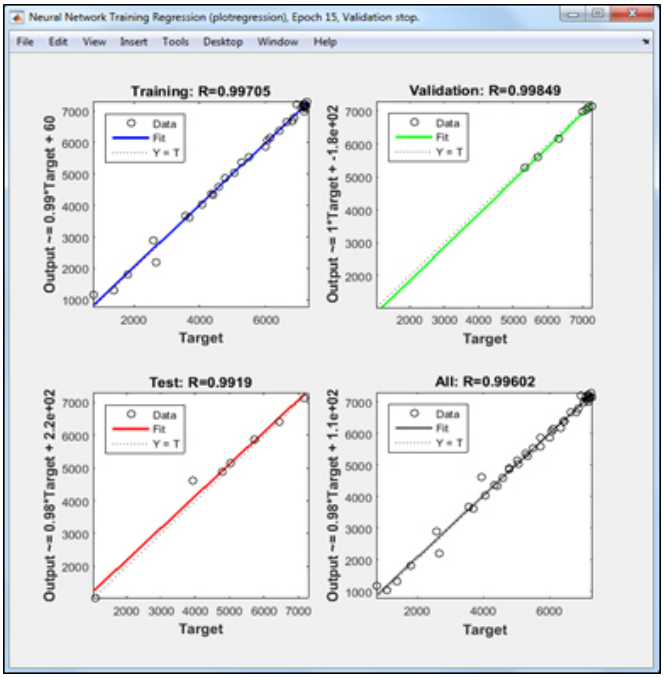

Fig. 9. Correlations of the NAR neural network

performance of the NARX model is observed during the testing phase. The NAR model shows a notable drop in the testing phase but recovers in the global coefficient. The Input-Output model performs very consistently, achieving outstanding performance in the testing phase and in the overall result.

Figure 14 represents the correlation values (r) in a visual format where differences are highlighted. The highest values are associated with the NARX and Input-Output models, especially in the validation and testing phases. The NAR model shows a visible discrepancy in the testing phase (lighter color), highlighting its lower performance compared to the

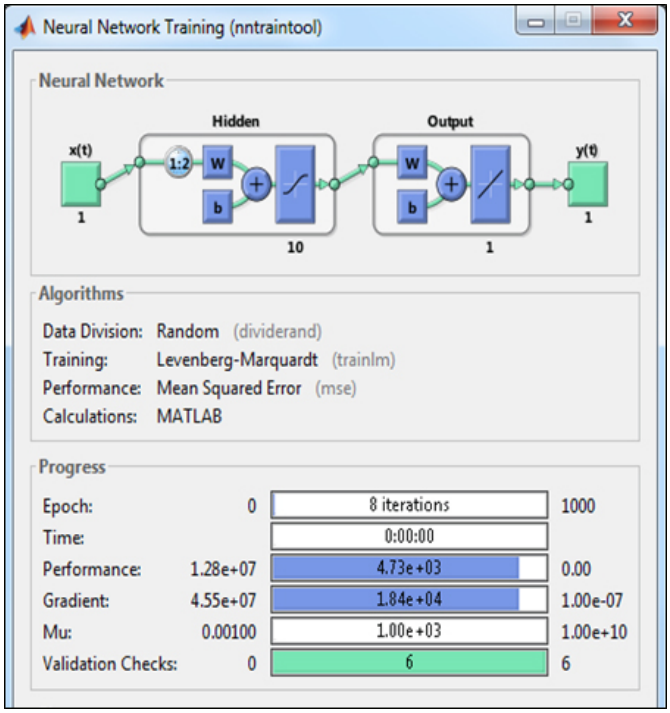

Fig. 10. Neural network training non linear Input – Output

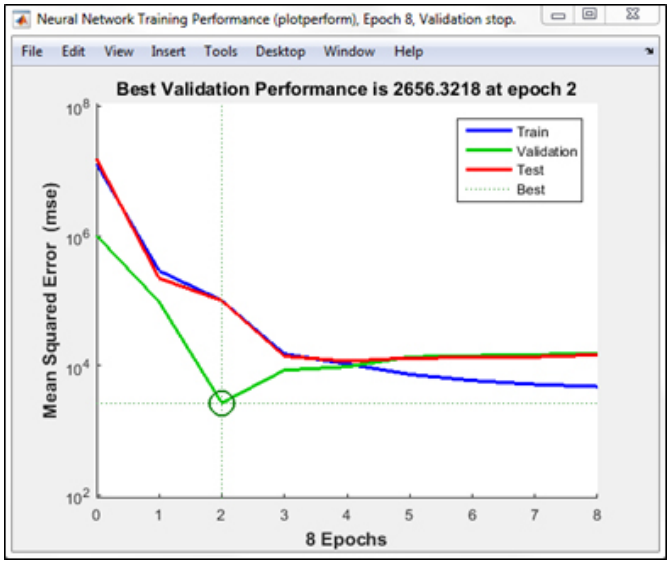

Fig. 11. Performance of the neural network non linear Input – Output

other models.

V. Conclusion

The NARX model has proven to be the most consistent and accurate, maintaining very high correlation coefficients across all phases. This positions it as the best option for predicting the thermal energy generated by vacuum flat plate solar collectors. The Input-Output model also delivers outstanding performance, especially in the testing phase where it reaches the highest value, suggesting it is highly reliable

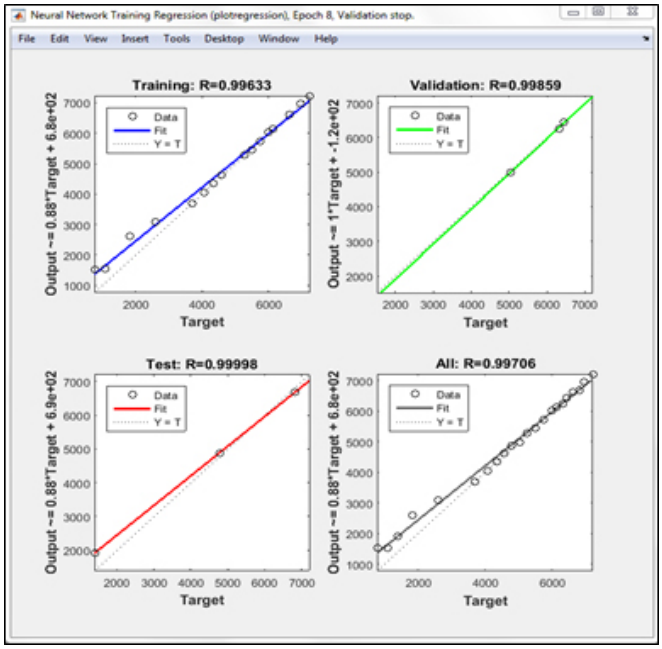

Fig. 12. Correlations of the neural network of non linear Input – Output

TABLE II
Comparative of the results of the three neural network models

Neural network	Models' training phase -(r)	Models' validation phase -(r)	Models' testing phase -(r)	Global correlation coefficient -(r)
NARX model	0.99993	0.99997	0.99777	0.99782
NAR model	0.99705	0.99849	0.9919	0.99602
Nonlinear Input-Output model	0.99633	0.99859	0.99998	0.99706

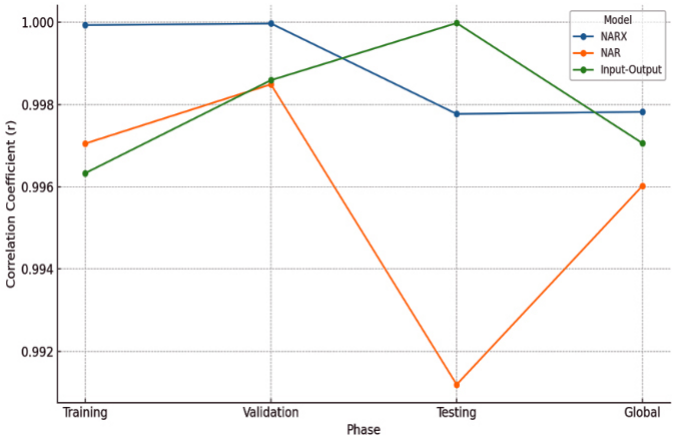

Fig. 13. Performance trends by phase

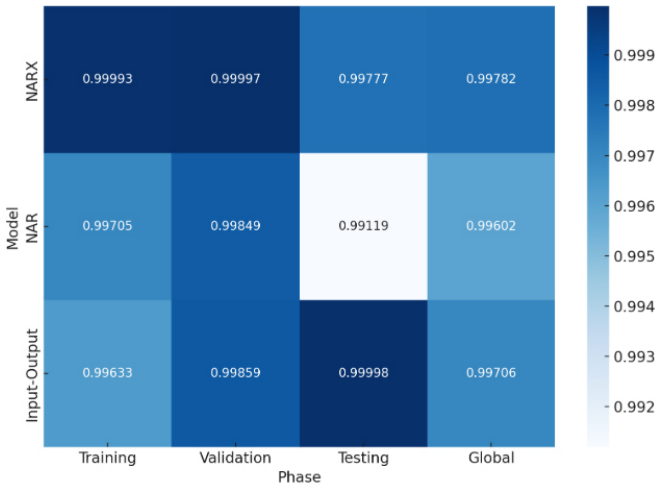

Fig. 14. Correlation of coefficients by phase and model

in practical prediction scenarios. Although the NAR model shows good overall performance, it demonstrates a noticeable decrease in the testing phase, which may indicate a lower ability to generalize on unknown data compared to the other models. If stability and overall accuracy are prioritized, the NARX model is the best option. However, if the goal is to find a model with the best performance in specific testing scenarios, the Input-Output model could be a valid alternative. The levels of prediction achieved can allow for more effective planning of energy generation, which is crucial for the efficient management of solar energy systems. This results in the optimization of available resources and better scheduling of equipment maintenance, which can reduce operating costs and extend the lifespan of the energy system components.

REFERENCES

[1] R. Gupta, A. K. Yadav, S. Jha, and P. K. Pathak, "Time series forecasting of solar power generation using Facebook prophet and XG boost," in Proc. IEEE Delhi Sect. Conf. (DELCON), Feb. 2022, pp. 1–5.

[2] M. Ramesh, A. K. Yadav, and P. K. Pathak, "Artificial gorilla troops optimizer for frequency regulation of wind contributed microgrid system," J. Comput. Nonlinear Dyn., vol. 18, no. 1, Jan. 2023, Art. no. 011005.

[3] P. K. Pathak, A. K. Yadav, A. Shastri, and P. A. Alvi, "BWOA assisted PIDF-(1+I) controller for intelligent load frequency management of standalone micro-grid," ISA Trans., vol. 132, pp. 387–401, Jan. 2023.

[4] M. Ramesh, A. K. Yadav, and P. K. Pathak, "Intelligent adaptive LFC via power flow management of integrated standalone micro-grid system," ISA Trans., vol. 112, pp. 234–250, Jun. 2021.

[5] P. K. Pathak, D. G. Roy, A. K. Yadav, S. Padmanaban, F. Blaabjerg and B. Khan, "A State-of-the-Art Review on Heat Extraction Methodologies of Photovoltaic/Thermal System," in IEEE Access, vol. 11, pp. 49738-49759, 2023, doi: 10.1109/ACCESS.2023.3277728.

[6] M. Pilz and L. Al-Fagih, "Selfish energy sharing in prosumer communities: A demand-side management concept," in Proc. IEEE Int. Conf. Commun., Control, Comput. Technol. Smart Grids (SmartGridComm), Piscataway, NJ, USA, Oct. 2019, pp. 1–6.

[7] N. L. Panwar, S. C. Kaushik, and S. Kothari, "Role of renewable energy sources in environmental protection: A review," Renew. Sustain. Energy Rev., vol. 15, no. 3, pp. 1513–1524, Apr. 2011.

[8] H.-W. Sinn, "Buffering volatility: A study on the limits of Germany's energy revofig," Eur. Econ. Rev., vol. 99, pp. 130–150, Oct. 2017.

[9] P. A. Schirmer, C. Geiger and I. Mporas, "Reducing Grid Distortions Utilizing Energy Demand Prediction and Local Storages," in IEEE Access, vol. 9, pp. 15122-15132, 2021, doi: 10.1109/ACCESS.2021.3053200.

[10] S. Lugo, L. I. Morales, R. Best, V. H. Gómez, and O. García-Valladares, "Numerical simulation and experimental validation of an outdoorswimming-pool solar heating system in warm climates," Solar Energy, vol. 189, no. 9, pp. 45–56, 2019.

[11] I. Mead, "International energy outlook 2017," US Energy Inf. Admin., Washington, DC, USA, 2017.

[12] B. N. Stram, "Key challenges to expanding renewable energy," Energy Policy, vol. 96, pp. 728–734, Sep. 2016.

[13] V. Sharma, A. Cortes and U. Cali, "Use of Forecasting in Energy Storage Applications: A Review," in IEEE Access, vol. 9, pp. 114690-114704, 2021, doi: 10.1109/ACCESS.2021.3103844.

[14] ASHRAE, Standard 1980 (RA 89) 1, 2003, p. 86244, vol. 6, no. Ra 89.

[15] J. Li, F. Liu, Z. Li, C. Shao, and X. Liu, "Grid-side flexibility of power systems in integrating large-scale renewable generations: A critical review on concepts, formulations and solution approaches," Renew. Sustain. Energy Rev., vol. 93, pp. 272–284, Oct. 2018.

[16] L. Che, X. Liu, X. Zhu, M. Cui, and Z. Li, "Assessment of dispatch intervals in power systems with high wind penetration," IEEE Trans. Sustain. Energy, to be published.

[17] S. Fan, Z. Li, Z. Li and G. He, "Evaluating and Increasing the Renewable Energy Share of Customers' Electricity Consumption," in IEEE Access, vol. 7, pp. 129200-129214, 2019, doi: 10.1109/ACCESS.2019.2940149.

[18] J. Yan, F. Li, Y. Liu, and C. Gu, "Novel cost model for balancing wind power forecasting uncertainty," IEEE Trans. Energy Convers., vol. 32, no. 1, pp. 318–329, Mar. 2017.

[19] M. A. Matos and R. J. Bessa, "Setting the operating reserve using probabilistic wind power forecasts," IEEE Trans. Power Syst., vol. 26, no. 2, pp. 594–603, May 2011.

[20] A. Botterud et al., "Demand dispatch and probabilistic wind power forecasting in unit commitment and economic dispatch: A case study of illinois," IEEE Trans. Sustain. Energy, vol. 4, no. 1, pp. 250–261, Jan. 2013.

[21] M. Shamsi and P. Cuffe, "Prediction Markets for Probabilistic Forecasting of Renewable Energy Sources," in IEEE Transactions on Sustainable Energy, vol. 13, no. 2, pp. 1244-1253, April 2022, doi: 10.1109/TSTE.2021.3112916.

[22] X. Qin, M. Gao, Z. He, and Y. Liu, "State of charge estimation for lithiumion batteries based on NARX neural network and UKF," in Proc. IEEE 17th Int. Conf. Ind. Informat. (INDIN), vol. 1. Finland: IEEE, Jul. 2019, pp. 1706–1711, doi: 10.1109/INDIN41052.2019.8972319.

[23] A. S. Ogundana, P. K. Terala, M. Y. Amarasinghe, X. Xiang and S. Y. Foo, "Electric Vehicle Battery State of Charge Estimation With an Ensemble Algorithm Using Central Difference Kalman Filter (CDKF) and Non-Linear Autoregressive With Exogenous Input (NARX)," in IEEE Access, vol. 12, pp. 33705-33719, 2024, doi: 10.1109/ACCESS.2024.3371883.

[24] H. Alouaoui, S. Turki, and S. Faiz, "A neural network based on time series for spatiotemporal relationships prediction," International Journal of Spatial, Temporal and Multimedia Information Systems, vol. 1, pp. 63–77, 2016, doi: 10.1504/IJSTMIS.2016.076785.

[25] M. R. C. Qazani, H. Asadi, C. P. Lim, S. Mohamed and S. Nahavandi, "Prediction of Motion Simulator Signals Using Time-Series Neural Networks," in IEEE Transactions on Aerospace and Electronic Systems, vol. 57, no. 5, pp. 3383-3392, Oct. 2021, doi: 10.1109/TAES.2021.3082662.

[26] R. Zemouri, R. Gouriveau, and N. Zerhouni, "Defining and applying prediction performance metrics on a recurrent NARX time series model," Neurocomputing, vol. 73, no. 13–15, pp. 2506–2521, Aug. 2010, doi: 10.1016/j.neucom.2010.06.005.

[27] M. Enqvist, "Linear Models of Nonlinear Systems," Ph.D. dissertation, Division of Automatic Control, Department of Electrical Engineering, Linköpings universitet, Linköping, Sweden, 2005.

[28] N. Benz and T. Beikircher, "High efficiency evacuated flat plate solar collector for process steam production," Solar Energy, vol. 65, pp. 111-118, 1999, doi: 10.1016/S0038-092X(98)00122-4.

[29] King Saud University, "ME 476 Solar Energy: Unit Four - Solar Collectors - Flat Plate Collectors," Faculty of Engineering, King Saud University, Riyadh, Saudi Arabia, 2023. [Online]. Available: faculty.ksu.edu.sa/ar

[30] S. J. Harrison, Q. Lin, and L. C. S. Mesquita, "Integral stagnation temperature control for solar collectors," in Proc. SESCI 2004 Conference, Waterloo, ON, Canada, Aug. 21-25, 2004, pp. ST-31.

[31] H. A. Al-Ansary, "Solar collectors - concentrating collectors," [Online]. Available: https://faculty.ksu.edu.sa/en/hansary/course-material/153300. [Accessed: Jan. 2025].